

Magnetic Phase Transitions in an $\text{Mn}_{0.9}\text{Co}_{0.1}\text{P}$ Single Crystal

Helmer Fjellvåg,^a Arne Kjekshus^{a,*} and Andrzej Zięba^b

^aDepartment of Chemistry, University of Oslo, N-0315 Oslo 3, Norway and ^bInstitute of Physics and Nuclear Techniques, Academy of Mining and Metallurgy, PL-30-059 Cracow, Poland

Fjellvåg, H., Kjekshus, A. and Zięba, A., 1990. Magnetic Phase Transitions in an $\text{Mn}_{0.9}\text{Co}_{0.1}\text{P}$ Single Crystal. – Acta Chem. Scand. 44: 8–11.

Results from a.c. magnetic susceptibility and strong field magnetization experiments are given for a single crystal of the pseudobinary phase $\text{Mn}_{0.9}\text{Co}_{0.1}\text{P}$ with an orthorhombic MnP-type structure. In zero field the para to ferro transition is observed at $T_C = 197$ K. The ferro to heli transition occurs below 63 K. The magnetic phase diagram for the applied field parallel to the intermediate axis of magnetization shows strong resemblance to that of pure MnP. This suggests that the triple point between the fan, ferro and heli phases in $\text{Mn}_{0.9}\text{Co}_{0.1}\text{P}$ may be a Lifshitz point.

Manganese monophosphide has been in scientific focus for a long time owing to its varied magnetic properties. Firstly, MnP was the first *compound* found to exhibit a double spiral magnetic structure.^{1,2} Secondly, detailed studies of single crystals of MnP with the magnetic field parallel to one of the three different orthorhombic axes revealed temperature (T) vs. magnetic field (H) phase diagrams with very interesting features,^{3–5} and one of the triple points (between the para-, ferro- and fan-magnetic phases) was shown to be the first physical manifestation of a Lifshitz point.^{6,7}

MnP also exhibits the ability to form solid solution phases easily with other 3d-metal monophosphides. Most of the other binary 3d-metal TP phases do not exhibit cooperative magnetism at low temperatures. For instance, CoP is a Pauli paramagnet, and upon substitution of CoP into MnP it is believed that the Co atoms act as simple, magnetically somewhat featureless diluents of the magnetic sublattice.^{8–10} The $\text{Mn}_{1-t}\text{Co}_t\text{P}$ phase diagram⁹ is shown in Fig. 1; as can be seen, both the ferromagnetic (F) regime (magnetic moments aligned along the a -axis; $Pm\bar{c}n$ setting of the unit cell) and the helimagnetic (H) regime of MnP extend into the ternary phase. Preliminary experiments on powder samples in magnetic fields show that $\text{Mn}_{1-t}\text{Co}_t\text{P}$ at low substitution levels (t) behaves in the same manner as MnP.^{8,9}

Ternary $\text{Mn}_{1-t}\text{Co}_t\text{P}$ samples are therefore very promising candidates for testing the effect of dilution on a modulated magnetic structure as well as the effect of dilution on a multicritical phenomenon such as the Lifshitz point. One expects no major complications due to magnetic interactions between solute and solvent, since Co, as mentioned above, seems to be a magnetically somewhat featureless diluent in $\text{Mn}_{1-t}\text{Co}_t\text{P}$. In this study we report magnetic phase diagrams found for single crystals of $\text{Mn}_{0.9}\text{Co}_{0.1}\text{P}$ for magnetic fields along the easy (c), intermediate (b) and

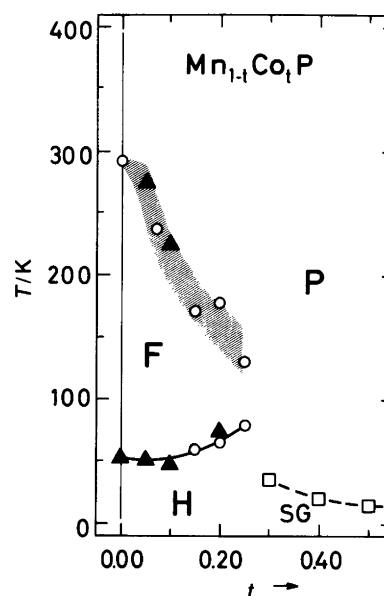


Fig. 1. Temperature–composition phase diagram for the $\text{Mn}_{1-t}\text{Co}_t\text{P}$ solid-solution phase.⁹ P denotes para-, F ferro- and H, helimagnetic phase regions.

hard (a) axes of magnetization. The results are discussed in relation to the corresponding phase diagrams for pure MnP.

Experimental

Single crystals of $\text{Mn}_{0.9}\text{Co}_{0.1}\text{P}$ were obtained by the Bridgman method. A bulk sample of the same composition was used as starting material, which in turn had been synthesized from MnP and CoP as described in Ref. 8. During the crystal pulling, the sample was kept inside a sealed, evacuated silica-glass ampoule which, prior to filling, had been coated with carbon.

* To whom correspondence should be addressed.

Following the crystal pulling, the Mn-Co-P ingot was cut into cubes with edges parallel to the three orthorhombic axes. The single crystal used in this study was a cube with all edges equal to 3.45 mm. The distribution of Mn/Co in the measured single crystal was examined by scanning electron microscopy (SEM) and Auger spectroscopy (SAM). The results confirmed the composition $\text{Mn}_{0.9}\text{Co}_{0.1}\text{P}$ and established that the actual single crystal specimen had no detectable concentration gradients. The overall Co content of the ingot was further verified by comparison of unit cell dimensions, and data obtained for cuts from the higher and lower parts of the ingot confirmed that concentration gradients were below the detection limit.

All magnetic measurements were performed using the same inductive magnetometer with a three-section pick-up coil inside the field coil. The single crystal was aligned in the sample holder with an angular accuracy of $\pm 1^\circ$. In the a.c. susceptibility measurements, an a.c. generator (300 Hz) was used, and the signals were measured by means of a lock-in voltmeter. Strong pulse fields were obtained by connecting the field coil to the capacitor bank. Temperatures down to 63 K were obtained by pumping on the liquid nitrogen reservoir.

Results and discussion

Like binary MnP itself, $\text{Mn}_{0.9}\text{Co}_{0.1}\text{P}$ crystallizes with the orthorhombic MnP-type structure. In this work, its unit cell is defined according to space group $Pm\bar{c}n$, whereas the standard setting of the cell is $Pnma$. The reason for this choice is that most important studies on the magnetic properties of MnP have been published according to the $Pm\bar{c}n$ setting, and in an attempt to avoid unnecessary confusion

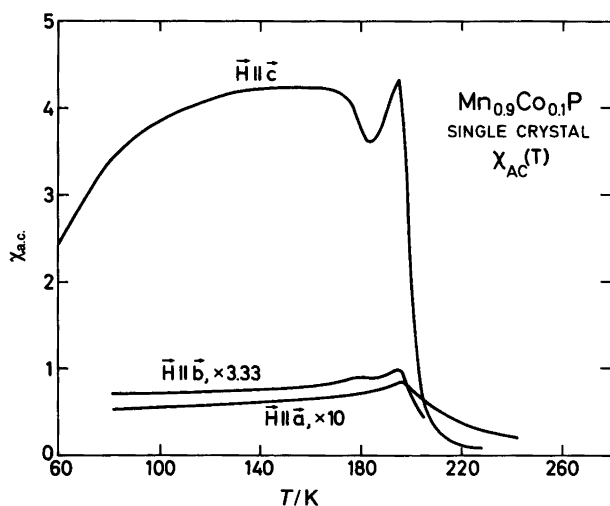


Fig. 2. Temperature dependence of the a.c. magnetic susceptibility of single crystals of $\text{Mn}_{0.9}\text{Co}_{0.1}\text{P}$, with the a.c. magnetic field parallel to, respectively, the a -, b - and c -axes (and zero d.c. external field). $\chi(T)$ plots for the external field parallel to b - and c -axes are magnified by a factor of 3.33 and 10, respectively.

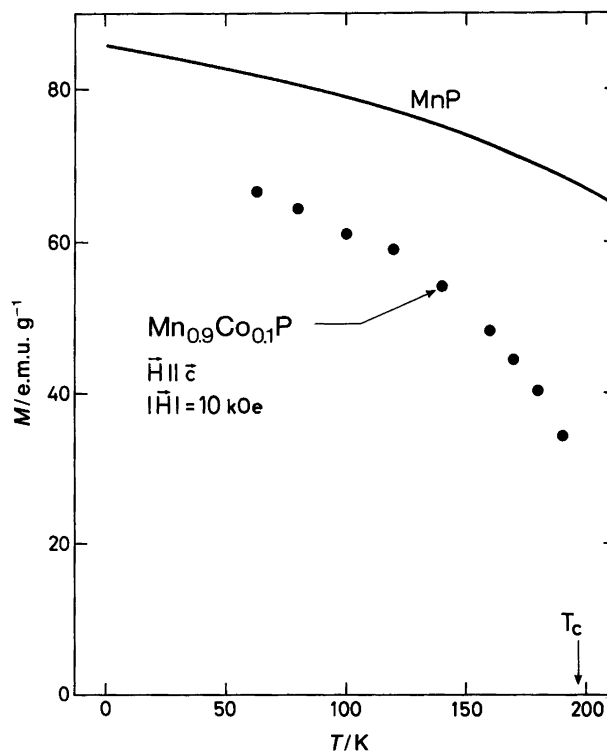


Fig. 3. Easy axis magnetization for a single crystal of $\text{Mn}_{0.9}\text{Co}_{0.1}\text{P}$. Data for MnP^{11} are included for comparison.

in the literature, the unconventional setting is maintained in this paper.

MnP is paramagnetic for temperatures above $T_C = 291$ K. Between T_C and $T_S = 50$ K MnP exhibits ferromagnetism with magnetic moments aligned parallel to the c -axis, whereas below T_S a double spiral occurs, propagating along the a -axis with the magnetic moments rotating in the bc -plane.¹⁻¹⁰ These basic features in zero magnetic field are also found for $\text{Mn}_{0.9}\text{Co}_{0.1}\text{P}$.^{8,9}

The results of a.c. magnetic susceptibility measurements for (a.c.) magnetic fields parallel to the three principal directions (i.e. along the crystallographic a -, b - and c -axes) are shown in Fig. 2. The susceptibilities represent effective values, i.e. dM/dH_{ext} with no correction for demagnetizing field. The large differences between the three curves clearly reflect the pronounced orthorhombic magnetic anisotropy of the structure, with c as the easy axis (χ_c is limited by the demagnetization), b as the intermediate axis and a as the hard axis of magnetization.

The ratios $\chi_c : \chi_b : \chi_a$ are larger than those reported for pure MnP.³ A comparison of the susceptibilities in Fig. 2 with χ_c of an MnP single crystal¹¹ and with measurements on powder samples reveals two novel features. Firstly, for χ_c there occurs a minimum just below T_C which was not seen for polycrystalline samples of $\text{Mn}_{1-x}\text{T}_x\text{P}$ ($T = \text{V}, \text{Cr}, \text{Fe}, \text{Co}, \text{Mo}$ and W ; but with a possible exception for $T = \text{Ni}$)^{9,10} or for single crystals of $\text{Mn}_{1-x}\text{Fe}_x\text{P}$.¹² Secondly, χ_c decreases progressively with decreasing temperature. This may be a precursor to the ferro- to helimagnetic transi-

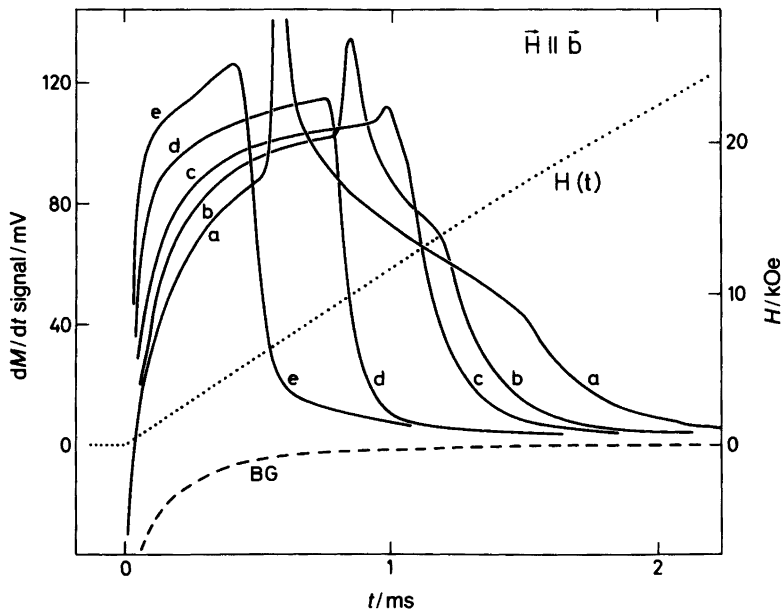


Fig. 4. Primary magnetometer signals dM/dt versus time (t) for an oriented single crystal of $Mn_{0.9}Co_{0.1}P$ with the magnetic field parallel to the intermediate axis (b). The time dependence of the background signal (BG; no sample) and the magnetic pulse field (H) are included. The curves refer to (a) 63, (b) 78, (c) 90, (d) 144 and (e) 180 K.

tion, which according to studies⁹ on powder samples of $Mn_{0.9}Co_{0.1}P$ occurs at around 50 K.

Easy axis of magnetization. At lower temperatures the magnetization along the easy (c) axis becomes saturated in a field of 5–10 kOe; close to T_C saturation is obtained in quite low fields. In Fig. 3 the magnetizations of $Mn_{0.9}Co_{0.1}P$ and MnP in a 10 kOe magnetic field are compared. At 63 K the decrease in magnetization of $Mn_{0.9}Co_{0.1}P$ is 18 % relative to MnP. This observation corresponds well with measured saturation moments⁹ at 4.2 K and in a field of 58 kOe for powder samples of $Mn_{1-t}Co_tP$, $0.00 \leq t \leq 0.25$.

The present $M(T, H)$ data for temperatures close to T_C show a critical scaling with non-classical exponents (the Arrot plots of $M^{1/\gamma}$ are definitely curved if classical exponents $\beta = 1/2$ and $\gamma = 1$ are assumed. However, for the non-classical values $\beta = 0.33$ and $\gamma = 1.30$ the curves become rather straight lines). The Arrot plot defines the Curie temperature as $T_C = 197$ K for $Mn_{0.9}Co_{0.1}P$. This fits reasonably well the value $T_C = 205$ K reported for powder samples with the same composition.^{8,9}

Intermediate axis of magnetization. For the intermediate (b) axis, the magnetization behaviour is also similar in $Mn_{0.9}Co_{0.1}P$ and MnP.^{6,7} Fig. 4 shows the primary pick-up coil signal dM/dt (which, owing to the nearly linear increase in magnetic field in the beginning of each field pulse, is approximately proportional to the differential susceptibility dM/dH) at various temperatures. The shape of the dM/dt curve indicates that two phase transitions occur at low temperatures. The sharp maximum corresponds, by analogy with MnP, to the ferro to fan transition, and the pronounced shoulder (at the high-field side) to the fan to para transition. At higher temperatures [curves (d) and (e)] these features merge and probably become indicative of the ferro to para transition.

The corresponding magnetic phase diagram is shown in Fig. 5. The triple point between the fan, ferro and para phases is found at $T_L = 97$ K and $H_L = 12.1$ kOe. In pure MnP this triple point exhibits the characteristics of a Lifshitz point. For $Mn_{0.9}Co_{0.1}P$ the triple point is found at values of both temperature and magnetic field that are some 25 % lower than for MnP. The triple point in $Mn_{0.9}Co_{0.1}P$ thus corresponds to the Lifshitz point in MnP.

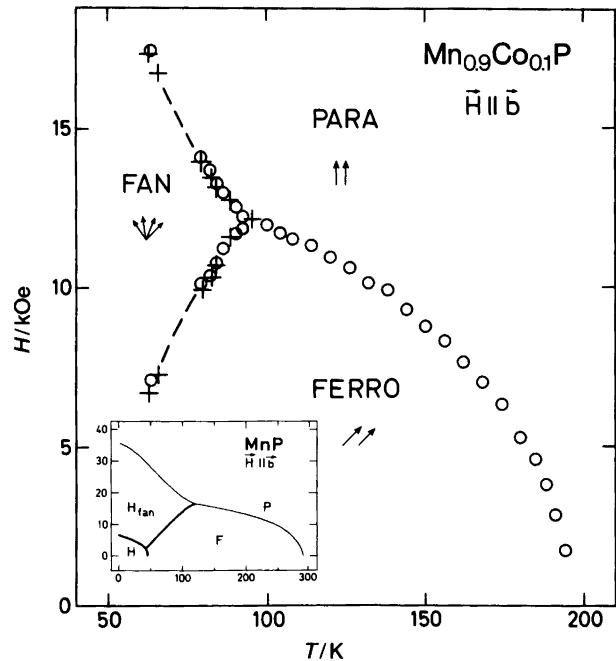


Fig. 5. High-temperature part of the magnetic phase diagram of $Mn_{0.9}Co_{0.1}P$ with the magnetic field parallel to the intermediate axis (b). Circles and crosses refer to experiments with maximum fields of 40 and 30 kOe, respectively. Insert shows corresponding phase diagram for MnP, quoted from Refs. 4–8.

Note that for the former composition the magnetic sublattice has been subjected to dilution. Detailed studies of the phase boundaries in the vicinity of the triple point, as well as detailed exploration by neutron diffraction of the variation of the wavevector characterizing the magnetic order in the fan phase, are in progress.

Hard axis of magnetization. For the hard (*a*) direction of the magnetization, approximate saturation at 77 K is obtained only for magnetic fields as high as 100 kOe. As opposed to the findings for the intermediate axis, the derivative dM/dH exhibits no clear features which can reasonably be attributed to magnetic phase transitions. Furthermore, rather large hysteresis effects are seen for increasing and decreasing field conditions. Only a diffuse maximum with a hardly noticeable shoulder is observed for increasing fields in the temperature interval just below T_C . For pure MnP, magnetic fields along the *a*-axis give rise to a magnetic phase diagram with a Lifshitz-type triple point between fan, ferro and para phases.⁷ However, for measurements with the magnetic field along the hard axis of magnetization careful alignment of the single crystal is of crucial importance. (The tolerance limit for the *b*-axis is larger.) It is likely that the observed, rather blurred dM/dH signal reflects a slight misalignment rather than indicating that the fundamental behaviour of $Mn_{0.9}Co_{0.1}P$ is quite different from that of the binary end-phase MnP.

An important question in all studies of phase transitions in disordered systems is whether the observed effects are merely due to inhomogeneities of the sample or if they represent genuine phenomena resulting from a homogeneous (random or preferred) distribution of the solute in the solvent. In the $Mn_{1-t}Co_tP$ solid-solution phase, the occurrence of two magnetic phase transitions (at T_C and T_S) is helpful in judging the quality of the samples, and to answer or comment on this question. The $Mn_{1-t}Co_tP$ phase is unique among the $Mn_{1-t}T_tP$ phases in that, while T_C drops considerably between $t = 0.00$ and 0.10 (from 291 to 197 K), T_S stays fairly constant. One thus expects that macroscopic inhomogeneities should produce a much larger smearing of T_C than of T_S . In fact, the observations (which are largely undocumented in this report) show the contrary. The small rounding of $\chi_{ac}(T)$ near T_C (Fig. 2) is further confirmed by successful Arrot plots of the $M(T, H)$ data. [Note that Aharoni¹³ has pointed out that $M^{1/\beta}$ versus

$(H/M)^{1/\gamma}$ becomes curved for an inhomogeneous system.] Another confirmation of the good quality of the present crystal is given by the strong anisotropy of the magnetic susceptibility (which is even larger than for pure MnP). The observation of a smearing of $\chi_{ac}(T)$ for $H \parallel c$ at low temperatures should consequently be taken as an indication of a real effect of disorder. We are at present not aware of any suitable theory for ferro- to helimagnetic transitions in disordered systems involving random exchange constants and random anisotropy. On the experimental side, more data are needed, both extending the temperature range of the present experiments to lower temperatures as well as improving the accuracy in the vicinity of the critical points.

Acknowledgements. This work has received financial support from the Norwegian Research Council for Science and the Humanities and the Polish programme CPBP 01.12. The skillful assistance of S. Lacher, *Max Planck Institut für Festkörperforschung*, Stuttgart, FRG in the crystal preparations is gratefully acknowledged.

References

1. Felcher, P. G. *J. Appl. Phys.* 37 (1966) 1056.
2. Forsyth, J. B., Pickart, S. J. and Brown, P. J. *Proc. Phys. Soc.* 88 (1966) 333.
3. Huber, E. E., Jr. and Ridgley, D. H. *Phys. Rev. A* 135 (1964) 1033.
4. Komatsubara, T., Suzuki, T. and Hirahara, E. *J. Phys. Soc. Jpn.* 28 (1970) 317.
5. Becerra, C. C., Missell, F. P., Oliveira, N. F., Jr. and Shapira, Y. *Phys. Stat. Sol. (a)* 22 (1974) K129.
6. Shapira, Y., Becerra, C. C., Oliveira, N. F., Jr. and Chang, T. S. *Phys. Rev. B* 24 (1981) 2780.
7. Shapira, Y., Oliveira, N. F., Jr., Becerra, C. C. and Foner, S. *Phys. Rev. B* 29 (1984) 361.
8. Fjellvåg, H. and Kjekshus, A. *Acta Chem. Scand., Ser. A* 38 (1984) 563.
9. Fjellvåg, H., Kjekshus, A., Zięba, A. and Foner, S. *J. Phys. Chem. Solids* 45 (1984) 709.
10. Zięba, A., Fjellvåg, H. and Kjekshus, A. *J. Phys. Chem. Solids* 49 (1988) 1087.
11. Takase, A. and Kasuya, T. *J. Phys. Soc. Jpn.* 47 (1979) 491.
12. Iwata, N., Fujii, H. and Okamoto, T. *J. Phys. Soc. Jpn.* 46 (1979) 778.
13. Aharoni, A. *J. Appl. Phys.* 56 (1984) 3479.

Received February 27, 1989.